nature communications

Article

https://doi.org/10.1038/s41467-025-62382-w

Neuropeptide Y neurons mediate opioid-induced itch by disinhibiting GRP-GRPR microcircuits in the spinal cord

Received: 8 October 2024

Accepted: 20 July 2025

Published online: 01 August 2025

Check for updates

Qian Zeng[1,2,5], Yitong Li[1,5], Yifei Wu[1,5], Jiawei Wu[1], Kangtai Xu[1], Yiming Chen[1], Yunfei Rao[1], Nan Li[2], Yuhui Luo[2], Changyu Jiang[2] ✉, Chaoran Wu[1] ✉ & Zilong Wang[1,3,4] ✉

Itch is a common side effect of opioid analgesics. The specific neurons mediating opioid-induced itch are still debated, and the mechanistic neuronal circuits remain elusive. Here, we show that the μ-opioid receptors (MOR) on neuropeptide Y (NPY)$^+$ inhibitory interneurons mediate opioid-induced itch at the spinal cord level in mice. The MOR gene *Oprm1* is expressed in NPY$^+$ neurons in the spinal dorsal horn, and specific deletion of *Oprm1* in NPY$^+$ interneurons abolishes intrathecal morphine-induced itch. Furthermore, gastrin-releasing peptide (GRP)$^+$ neurons are the direct downstream targets of NPY$^+$ neurons. Mechanistically, morphine inhibits the neuronal excitability of NPY$^+$ interneurons and reduces inhibitory synaptic inputs on GRP$^+$ neurons, causing disinhibition of GRP$^+$ neurons and further activation of gastrin-releasing peptide receptor (GRPR)$^+$ neurons. The NPY/neuropeptide Y receptor 1(NPY1R) system is essential for regulating GRP$^+$ neurons in opioid-induced itch. These findings reveal that intrathecal opioids act on MOR on NPY$^+$ inhibitory neurons in the spinal dorsal horn, which subsequently disinhibit GRP-GRPR microcircuits, triggering the itch response.

Opioid drugs are the most commonly used analgesics for treating moderate to severe pain in clinics[1]. While playing a major role in opioid analgesics[2–4], the μ-opioid receptor (MOR) can lead to unwanted side effects, such as respiratory inhibition, addiction, and opioid-induced constipation[2,5,6], due to its broad expression in the nervous system. Pruritus is another common side effect of opioid analgesics. Clinical research reported that pruritus occurs in 30–100% of cases following epidural or intrathecal administration of opioid analgesics[7,8]. On the other hand, MOR antagonists, like naloxone, naltrexone, and nalbuphine, have proven effective in mitigating chronic itch associated with dermatitis, cholestatic liver disease, uremic disease, or programmed cell death protein 1(PD1) immunotherapy[9–11]. Despite numerous studies on the mechanism of itch sensation generation in both peripheral and central nervous systems, the nature of MOR signaling in itch transmission is not fully elucidated.

Itch transmission at the spinal cord level has been well-documented in recent studies[12–15]. Based on the peripheral inputs, itch can be classified into chemical and mechanical types. Chemical pruritogens activate pruriceptive sensory neurons, which send itch signals to spinal natriuretic peptide receptor-A (NPRA)$^+$ neurons via natriuretic polypeptide b (Nppb)[16,17]. Activation of secondary sensory neurons, either NPRA$^+$ or gastrin-releasing peptide (GRP)$^+$,

[1]Department of Medical Neuroscience, School of Medicine; Shenzhen People's Hospital, The First Affiliated Hospital; Southern University of Science and Technology, Shenzhen, Guangdong, China. [2]Department of Pain Medicine and Shenzhen Municipal Key Laboratory for Pain Medicine, The 6th Affiliated Hospital of Shenzhen University Medical School, Shenzhen, Guangdong, China. [3]Key University Laboratory of Metabolism and Health of Guangdong School of Medicine, Southern University of Science and Technology, Shenzhen, Guangdong, China. [4]SUSTech Homeostatic Medicine Institute, SUSTech Center for Pain Medicine, School of Medicine, Southern University of Science and Technology, Shenzhen, Guangdong, China. [5]These authors contributed equally: Qian Zeng, Yitong Li, Yifei Wu. ✉e-mail: changyujiang@email.szu.edu.cn; wu.chaoran@szhospital.com; wangzl6@sustech.edu.cn

subsequently relays itch signals to gastrin-releasing peptide receptor (GRPR)$^+$ neurons to elicit itch[18–20]. Furthermore, neuropeptide Y (NPY)$^+$ inhibitory interneurons and dynorphin$^+$ inhibitory interneurons were demonstrated to gate control the itch circuits in the spinal dorsal horn (SDH)[21–28]. The spinal chemical itch circuit is gated by spinal dynorphin$^+$ inhibitory interneurons, which inhibit GRPR$^+$ neurons[25]. For mechanical itch, light touch stimuli activate low threshold mechanical receptors (LTMRs), which transmit the mechanical itch information to spinal neuropeptide Y receptor 1 (NPY1R)$^+$ or Urocortin 3 (Ucn3)$^+$ neurons, and these neurons are gated by spinal NPY$^+$ inhibitory neurons[22,23,29]. Interestingly, recent studies have demonstrated that NPY$^+$ inhibitory interneurons regulate not only mechanical itch but also chemical itch[21,29,30].

While emerging evidence suggests that the MOR on spinal inhibitory interneurons plays a key role in regulating opioid-induced pruritus and some forms of chronic pruritus[4,31,32], the detailed mechanisms are largely enigmatic, and current findings lack consistency. For example, Nguyen et al. reported that morphine induces itch by acting on MOR on dynorphin$^+$ inhibitory interneurons of the spinal cord[32]. Yet, Wang et al. suggested that not only dynorphin$^+$ neurons, but also NPY$^+$ neurons express MOR in the dorsal horn of the spinal cord, and more importantly, intrathecal NPY almost eliminated morphine-induced itch[4]. These observations underscore the complexity of inhibitory interneuron subtypes involved in opioid-induced itch. Here, we extended our prior research on NPY's inhibition of morphine-induced itch to determine the involvement of NPY$^+$ neurons and their downstream neural circuits in scratching behaviors evoked by morphine. This study found that morphine-induced itch was abolished in mice with specific deletion of *Oprm1* on NPY$^+$ inhibitory interneurons (*Npy^{Cre};Oprm1$^{fl/fl}$*). MOR activation on NPY$^+$ interneurons led to a decrease in their neuronal excitability, which subsequently disinhibited GRP$^+$ excitatory interneurons and triggered itch responses. Furthermore, the NPY-NPY1R system was demonstrated to regulate the activities of GRP$^+$ interneurons in mediating opioid-induced itch.

Results

MOR on NPY$^+$ inhibitory interneurons in SDH is required for opioid-induced itch

Our recent study indicated that MOR on inhibitory neurons mediates morphine-induced itch via disinhibition[4]. To extend this finding, we first examined *Oprm1* expression in the SDH by RNAscope in situ hybridization. There were 38.27% *Oprm1*$^+$ interneurons expressing *Npy* and 29.96% of NPY$^+$ interneurons expressing *Oprm1* (Figs. 1A, B and S1A), consistent with previous reports[4,32]. The specific staining of the RNAscope probe was confirmed by positive and negative probes (Fig. S1B–D). This result suggests that *Oprm1* in inhibitory interneurons is markedly expressed in NPY$^+$ interneurons in the SDH. Next, chemogenetic activation of NPY$^+$ interneurons was used to evaluate whether the NPY$^+$ interneurons contribute to morphine-induced itch (Fig. S2A). Chemogenetic activation of spinal NPY$^+$ interneurons by intrathecal injection of CNO abolished intrathecal morphine-induced itch response in *Npy^{Cre};hM3Dq* mice, suggesting that NPY$^+$ interneurons contribute to the morphine-induced scratching response (Fig. 1C, $t = 3.722$, $P = 0.0029$). Biting and licking towards the hind paw or the tail after intrathecal morphine injection may reflect an itch response to the hindquarters[33]. Chemogenetic activation of NPY$^+$ interneurons also eliminated morphine-induced biting and licking behaviors (Fig. S2B, $t = 2.869$, $P = 0.0141$). Next, we generated *Oprm1* condition knockout mice (*Npy^{Cre};Oprm1$^{fl/fl}$*) by crossing *Npy^{Cre}* mice with *Oprm1$^{fl/fl}$* mice to assess the functional roles of MOR on NPY$^+$ interneurons in morphine-induced itch. RNAscope results validated *Oprm1* conditional knockout in NPY$^+$ interneurons (Fig. S2C, D, $t = 15.05$, $P < 0.0001$). Strikingly, these mice exhibited complete loss of scratching behaviors in response to different doses of morphine (Fig. 1D, $F(1, 48) = 37.80$, $P = 0.1336$, $P = 0.0005$, $P < 0.0001$, respectively). Morphine-induced biting and licking were also eliminated in these mice (Fig. S2E, $F(1, 48) = 13.11$, $P > 0.9999$, $P = 0.0664$, $P = 0.0026$, respectively). We next used endomorphin-1 (EM-1), a MOR-selective endogenous ligand, to evaluate whether MOR on NPY$^+$ interneurons mediates endogenous opioid-induced itch. Intrathecal EM-1 elicited a dose-dependent, short-term scratch behavior within the first 5 min in wild-type (WT) mice (Fig. 1E, $F(4, 33) = 7.736$, $P = 0.8586$, $P = 0.4057$, $P = 0.0018$, $P = 0.0002$, respectively). Similar to morphine, EM-1-induced itch was also completely abolished in mice with conditional deletion of *Oprm1* in NPY$^+$ interneurons (Fig. 1F, $t = 2.675$, $P = 0.0160$). These results indicate that MOR on NPY$^+$ interneurons mediates both endogenous and exogenous MOR agonists-evoked itch.

Next, we performed ex vivo electrophysiology recordings of spinal cord slices to evaluate the effects of morphine on NPY$^+$ interneuron activity. *Npy^{Cre}*;Ai9 tdTomato reported mice were used to label NPY$^+$ interneurons. Opioids activate potassium channels through G protein to generate outward currents in MOR-expressing neurons[34]. Our recording data showed that morphine (10 μM) evokes outward currents in 17 of 34 SDH lamina I-II NPY$^+$ interneurons with an average amplitude of 16.84 pA (Fig. 2A, B). The response rate closely matched our RNAscope double labeling results, confirming functional MOR expression on NPY$^+$ interneurons. Furthermore, morphine significantly inhibited evoked action potentials in 9 out of 22 SDH lamina II NPY$^+$ interneurons (Fig. 2C–E, $F(1, 8) = 40.26$, $P = 0.0002$). Our recording data showed that morphine perfusion notably increased rheobase, the minimum current required to evoke an action potential, in NPY$^+$ interneurons (Fig. 2F, $t = 3.043$, $P = 0.0160$). In contrast, vehicle perfusion did not change action potentials and rheobase (Fig. 2G–I, $F(1, 8) = 0.01969$, $P = 0.8919$; $t = 0.7365$, $P = 0.4825$, respectively). These results indicate that morphine decreases the excitability of NPY$^+$ interneurons via MOR expressed on these neurons, which may further disinhibit the itch circuit and elicit an itch response.

NPY-NPY1R system regulates opioid-induced itch

Given the established role of NPY and NPY1 receptor (NPY/NPY1R) system in itch transmission[23,29], we next tested whether NPY directly regulates intrathecal morphine-induced itch. Co-injection of NPY significantly attenuated morphine-induced scratching or biting behaviors in a dose-dependent manner (Fig. 3A, $F(3, 31) = 4.664$, $P = 0.1131$, $P = 0.0242$, $P = 0.0055$, respectively; Fig. S3A, $F(3, 31) = 13.24$, $P = 0.0531$, $P = 0.0009$, $P < 0.0001$, respectively). These behaviors were also suppressed by different doses of [Leu^{31}, Pro^{34}] NPY (LP-NPY), a specific agonist of the NPY1R (Fig. 3B, $F(3, 33) = 12.47$, $P = 0.0125$, $P = 0.0019$, $P < 0.0001$, respectively; Fig. S3B, $F(3, 33) = 11.85$, $P = 0.0002$, $P < 0.0001$, $P < 0.0001$, respectively). The specificity of their effects was confirmed because the impact of LP-NPY on morphine-induced itch was completely blocked by the NPY1R selective antagonist BIBO3304 (Fig. 3C, $F(3, 36) = 13.42$, $P < 0.0001$), and NPY failed to reduce morphine-induced itch in *Npy1r* global knockout (*Npy1r$^{-/-}$*) mice (Fig. 3D, $F(3, 34) = 3.353$, $P = 0.9851$). In addition, targeted deletion of *Npy1r* in global knockout mice was validated by the absence of *Npy1r* gene expression in SDH as determined by q-PCR (Fig. S3C, $t = 5.015$, $P = 0.0015$) and RNAscope (Fig. S3D, E, $t = 9.844$, $P < 0.0001$). These data suggested that NPY$^+$ neurons might have tonic inhibition on itch circuits by releasing NPY. However, *Npy1r$^{-/-}$* mice did not show significant spontaneous itch (Fig. S3F, $t = 0.7166$, $P = 0.4854$). This may be due to the compensation of global knockout mice. However, intrathecal injection of NPY1R antagonist BIBO3304 showed rapid and short-term itch behavior within the first 5 min (Fig. S3G, $F(1, 96) = 6.812$, $P < 0.0001$). Furthermore, to test whether the NPY-NPY1R system is involved in endogenous opioid-induced itch, we examined the effects of intrathecal NPY and LP-NPY on EM-1-induced itch. The results showed that both of them significantly inhibited EM-1-induced itch (Fig. 3E, $t = 2.640$, $P = 0.0247$; Fig. 3F, $t = 3.173$, $P = 0.0068$). These

https://doi.org/10.1038/s41467-025-62382-w

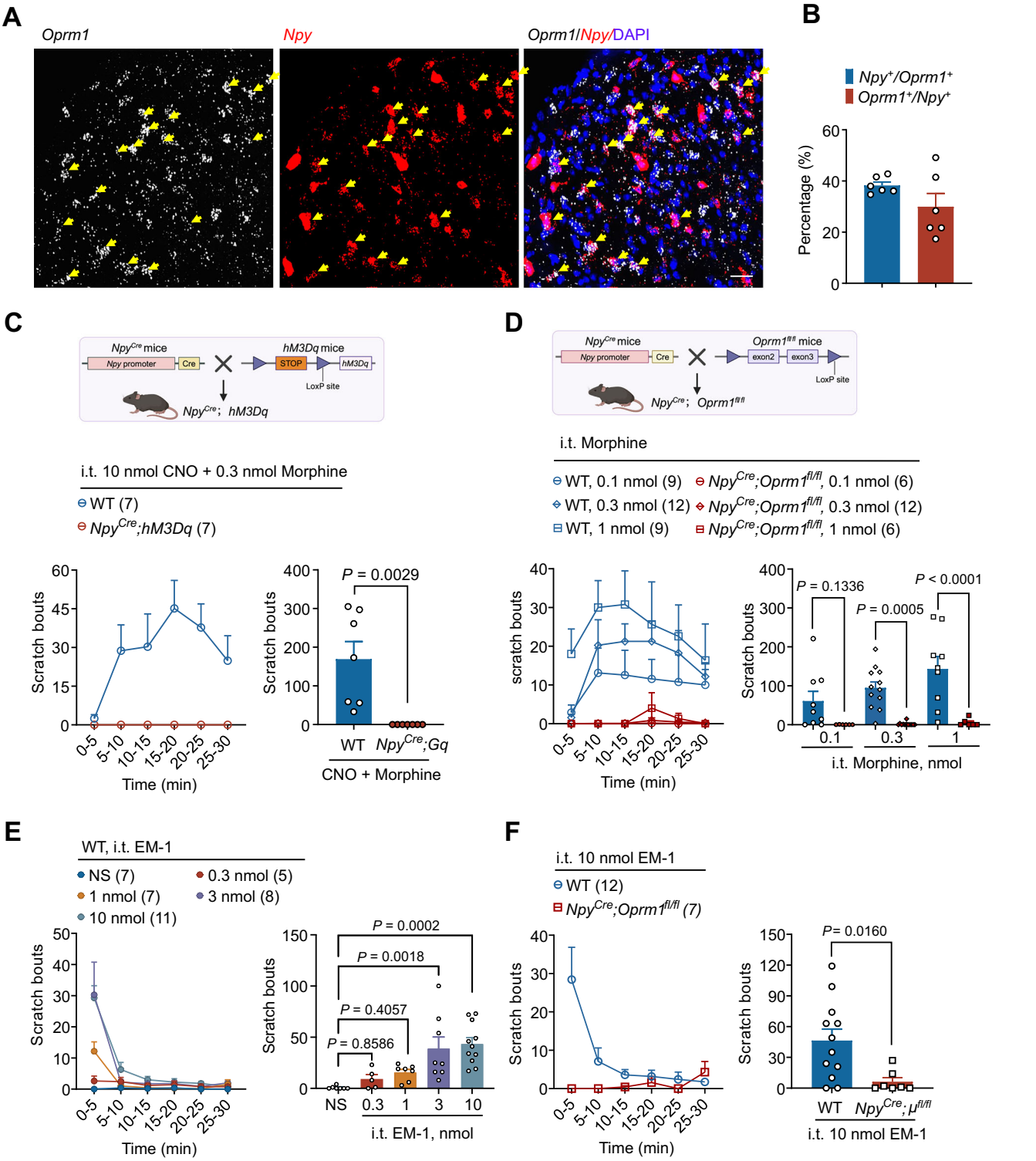

Fig. 1 | Opioid-induced itch is mediated by MOR on the NPY^{+} interneurons. A In situ hybridization RNAscope images of MOR mRNA (*Oprm1*, white) and NPY mRNA (*Npy*, red) in mouse spinal dorsal horn (SDH). Yellow arrows indicate *Oprm1* double-labeled with *Npy*, cells containing ≥ 5 RNAscope puncta were considered positive expression. Scale bar = 20 μm. **B** The percentage of co-expression between MOR and NPY neurons in the SDH, 12 spinal cord sections from 6 mice were analyzed. **C** Time course (left) and total scratch bouts (right) following intrathecal injection 10 nmol CNO (30 min before) and 0.3 nmol morphine in *Npy^{Cre};hM3Dq* or WT mice, student's unpaired two-tailed *t*-test. **D** Time course (left) and total scratch bouts (right) after intrathecal injection of 0.1, 0.3, 1 nmol morphine in *Npy^{Cre};Oprm1$^{fl/fl}$* mice, two-way ANOVA, Bonferroni's multiple comparisons. **E** Time course (left) and total scratch bouts (right) after intrathecal injection of various doses of EM-1 (0.3, 1, 3, 10 nmol) in WT mice. One-way ANOVA, Dunnett's multiple comparisons. **F** Intrathecal EM-1 (10 nmol)-induced scratching was significantly inhibited in *Npy^{Cre};Oprm1$^{fl/fl}$* mice, student's unpaired two-tailed *t* test. Data are shown as means ± SEM. *P* values are indicated in the figures. Sample sizes are presented in parentheses. Source data are provided as a Source Data file. Created in BioRender. Wang, Z. (2025) https://BioRender.com/u0x7q3a.

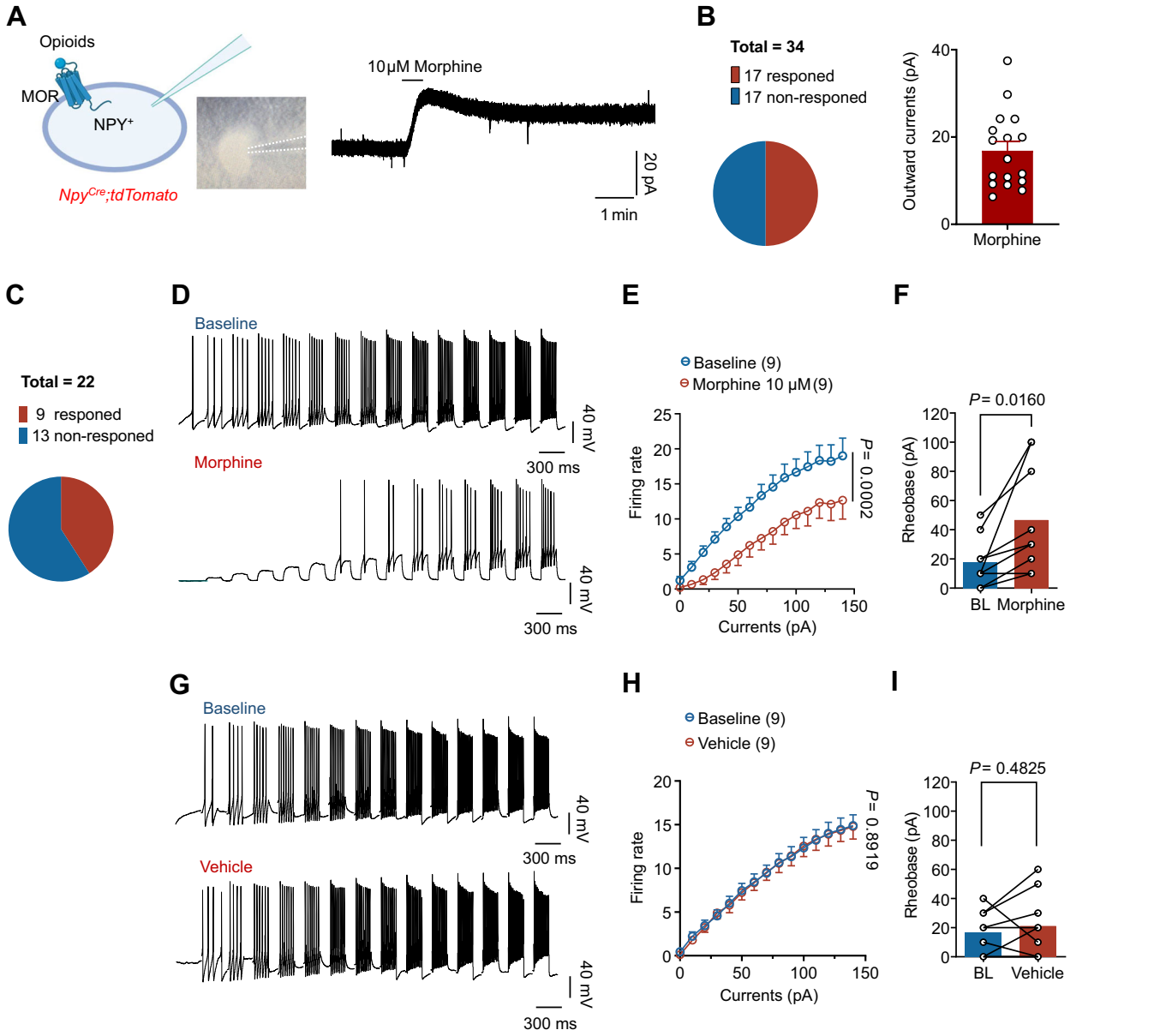

Fig. 2 | Morphine inhibits the excitability of NPY$^+$ inhibitory interneurons in the SDH. A Morphine (10 μM)-induced outward currents were recorded from NPY$^+$ interneurons in the SDH from *Npy^{Cre};tdTomato* mice. **B** Fifty percent of recorded neurons (17/34) showed outward currents with an average current of 16.85 pA. 34 neurons from 4 mice were analyzed. Data are shown as means ± SEM. **C** Morphine (10 μM) significantly reduced action potentials in the 9/22 recorded NPY$^+$ interneurons. 22 neurons from 4 mice were analyzed. **D** Representative traces of action potentials before and after morphine treatment. **E** Quantifications of the effects of morphine on action potentials, two-way ANOVA, Bonferroni's multiple comparisons. Data are shown as means ± SEM. **F** Quantifications of the rheobase, paired two-tailed *t*-test. 9 neurons from 4 mice were analyzed. Data are shown as means with dots. **G** Representative traces of action potentials before and after vehicle treatment. **H** Quantifications of the effects of the vehicle on action potentials, two-way ANOVA, Bonferroni's multiple comparisons. Data are shown as means ± SEM. **I** Quantifications of the rheobase, paired two-tailed *t*-test. 9 neurons from 3 mice were analyzed. Data are shown as means with dots. *P* values are indicated in the figures. Sample sizes are presented in parentheses. Source data are provided as a Source Data file. Created in BioRender. Wang, Z. (2025) https://BioRender.com/f0vl0vl.

data suggest that NPY directly regulates opioid-induced itch response via NPY1R.

GRP$^+$ interneurons are the direct downstream of NPY$^+$ interneurons and mediate opioid-induced itch

We proceeded to investigate the downstream itch-related neuron types activated by the disinhibition of MOR-expressed NPY$^+$ interneurons. First, the data from detecting neuronal activation marker gene *c-Fos* showed that intrathecal injected morphine significantly activates both *Grp*$^+$ and *Grpr*$^+$ neurons (Figs. 4A, D and S4A, B). Further analysis showed a significant increase in the *c-Fos* positive neurons after intrathecal injection of morphine in *Grp*$^+$ neurons in SDH (Fig. 4B, $F(2, 16) = 17.11$, $P = 0.0002$). However, a significant decrease in the *c-Fos* positive neurons was observed after intrathecal co-injection of morphine and NPY (Fig. 4B, $F(2, 16) = 17.11$, $P = 0.0008$). Only 4.35% of *Grp*-labelled cells in the lamina II of SDH displayed *c-Fos* signals in the saline group, but this was dramatically increased to 18.59% in the morphine-treated group (Fig. 4C, $F(2, 16) = 16.53$, $P = 0.0004$). Furthermore, it was significantly decreased to 5.28% by co-administration of NPY (Fig. 4C, $P = 0.0004$). In addition, the *c-Fos* positive neurons in the lamina I-II of SDH were also significantly increased in *Grpr*$^+$ neurons (Fig. 4E, $F(2, 16) = 10.61$, $P = 0.0009$) and notably decreased after

https://doi.org/10.1038/s41467-025-62382-w

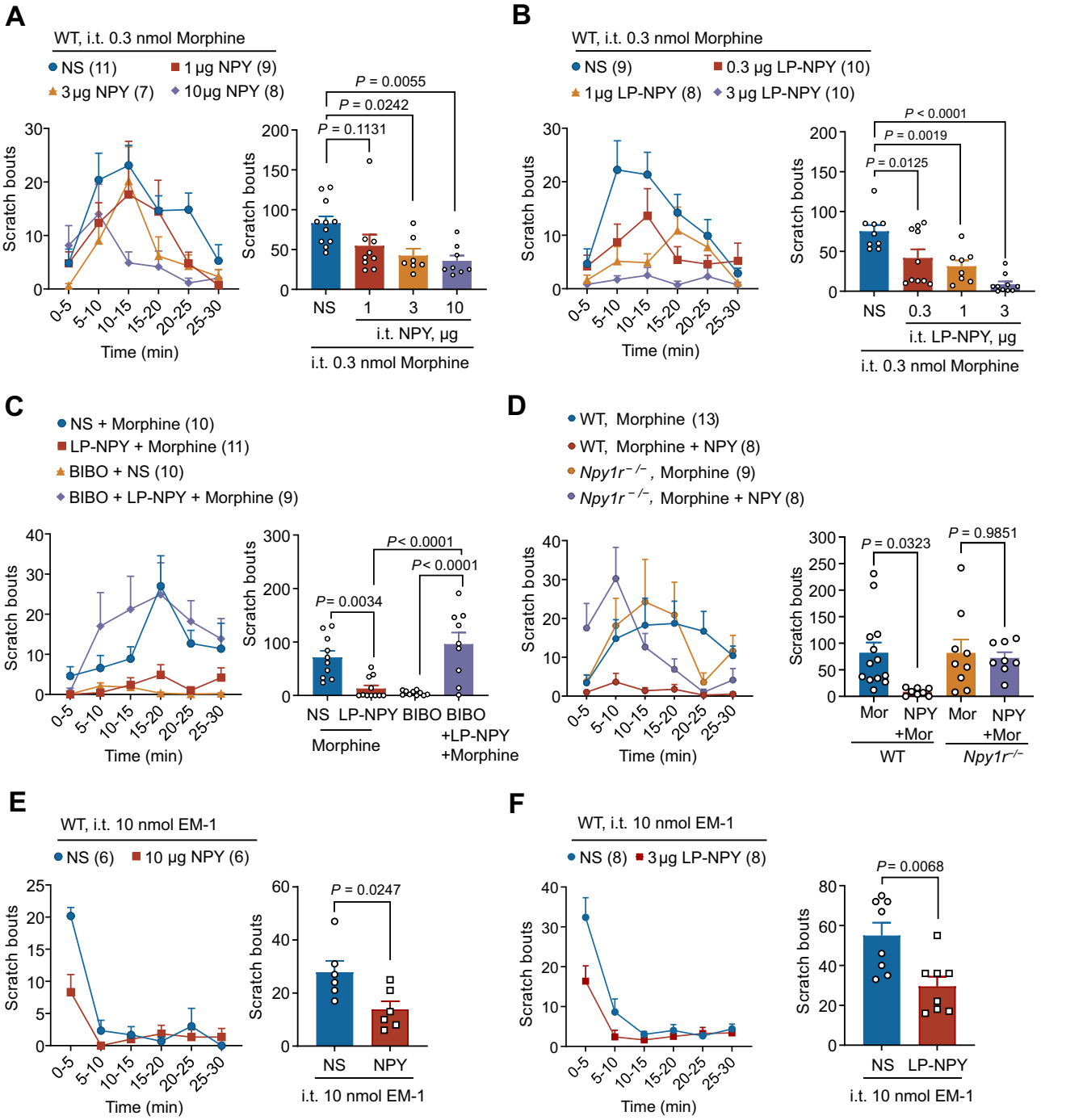

Fig. 3 | NPY-NPY1R is involved in intrathecal opioid-induced itch. A Intrathecal morphine-induced scratching was dose-dependently inhibited by co-injection with NPY (1, 3, 10 μg), one-way ANOVA, Dunnett's multiple comparisons. **B** Intrathecal morphine-induced scratching was significantly attenuated by co-injection with NPY1R selective agonist [Leu^{31}, Pro^{34}] NPY (LP-NPY) (0.3, 1, 3 μg), one-way ANOVA, Dunnett's multiple comparisons. **C** Intrathecal injection of NPY1R selective antagonist BIBO3304 (BIBO, 10 μg, 20 min before) blocked the effects of LP-NPY (3 μg) on morphine-induced itch, one-way ANOVA, Dunnett's multiple comparisons. **D** Intrathecal co-injected morphine (0.3 nmol) and NPY (10 μg) in WT or *Npy1r*$^{-/-}$ mice, one-way ANOVA, Dunnett's multiple comparisons. **E** Intrathecal EM-1 (10 nmol)-induced scratching was inhibited by 10 μg NPY, student's unpaired two-tailed *t*-test. **F** Intrathecal EM-1 (10 nmol)-induced scratching was inhibited by 3 μg LP-NPY, student's unpaired two-tailed *t*-test. Data are shown as means ± SEM. *P* values are indicated in the figures. Sample sizes are presented in parentheses. Source data are provided as a Source Data file.

morphine plus NPY treatment (Fig. 4E, $P = 0.0135$). Following morphine treatment, the *c-Fos* positive percentage increased to 16.46% from 6.73% in *Grpr*-labelled cells in the SDH (Fig. 4F, $F(2, 16) = 6.085$, $P = 0.0059$). To further determine the direct downstream neuron type of NPY^{+} interneurons, *Npy*^{Cre} mice were intraspinally injected (T_{13}-L_1 levels) into the SDH with rAAV-CAG-DIO-mWGA-mCherry virus, which is a Cre-dependent fluorescent wheat germ agglutinin (WGA) based anterograde synaptic tracer (Fig. 4G)[35]. The data showed that the WGA-mCherry signal is expressed in both NPY^{+} and GRP^{+} interneurons, but only a few in GRPR^{+} interneurons, indicating that NPY^{+} interneurons provide synaptic inputs onto GRP^{+} interneurons (Fig. 4H–J, $t = 4.315$, $P = 0.0125$, Fig. S4C, D). A previous study reported that WGA can move

https://doi.org/10.1038/s41467-025-62382-w

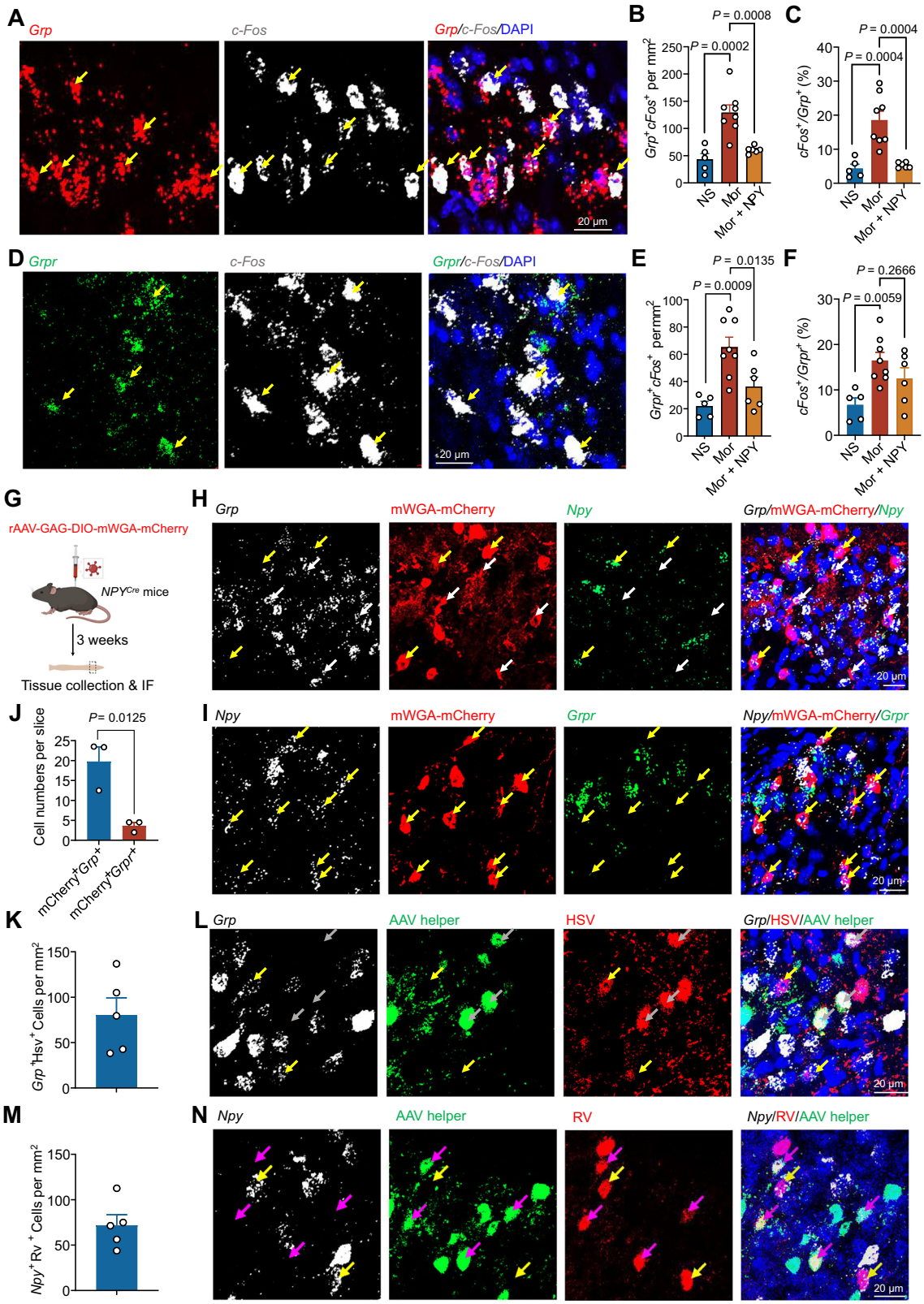

over several synapses[36]. The WGA in GRPR$^+$ neurons might be the result of the WGA moving over two synapses or a few GRPR$^+$ neurons receiving a direct synapse connection from NPY$^+$ neurons. To further confirm the synaptic connection between NPY$^+$ and GRP$^+$ interneurons. We used herpes simplex virus (HSV)-anterograde tracer and rabies virus (RV)-retrograde tracer. We injected HSV labeled with the red fluorescent protein (HSV-mCherry) following the expression of adeno-associated virus (AAV) helpers rAAV-hSyn-DIO-EGFP-T2A-Her2CT9 and rAAV-UL26.5-DIO-gD in the lumbar spinal cord of *Npy*^{Cre} mice (Fig. S5A)[37]. We observed mCherry-positive neurons in *Grp*$^+$ interneurons by RNAscope (Figs. 4K, L and S5B). Then, the RV retrograde tracing was used to examine whether GRP$^+$ neurons receive NPY$^+$ neuron inputs. We intraspinally injected (T_{13}-L_1 levels) AAV helpers rAAV-EF1α-DIO-EGFP-T2A-TVA and rAAV-EF1α-DIO-N2cG 14 days before, then intraspinally

Fig. 4 | GRP$^+$ interneurons are the direct downstream targets of NPY$^+$ interneurons with monosynaptic connections. **A**–**F** *c-Fos* expression in the SDH after intrathecal injected saline (15 spinal cord sections from 5 mice were analyzed) or morphine (0.3 nmol, 23 spinal cord sections from 8 mice were analyzed) or morphine + NPY (0.3 nmol + 10 μg, 18 spinal cord sections from 6 mice were analyzed) in WT mice, one way ANOVA, Dunnett's multiple comparisons (**B**–**E**). **A** Co-expression of *Grp* (red) and *c-Fos* (white) mRNA in the SDH after intrathecal injection of morphine. Yellow arrows indicate *Grp* double-labeled with *c-Fos*. **B** The cell numbers of *Grp* and *c-Fos* double-positive neurons in the SDH. **C** The ratio of *c-Fos*$^+$ neurons in *Grp*$^+$ neurons. **D** Co-expression of *Grpr* (Green) and *c-Fos* (White) mRNA in the SDH after intrathecal injected morphine. Yellow arrows indicate *Grpr* double-labeled with *c-Fos*. **E** The cell numbers of *Grpr* and *c-Fos* double-positive neurons in the SDH. **F** The ratio of *c-Fos*$^+$ neurons in *Grpr*$^+$ neurons. **G** Spinal dorsal horn injection of rAAV-CAG-DIO-mWGA-mCherry virus in *Npy*^{Cre} mice. **H** mWGA-mCherry signals were detected in both *Npy*$^+$ (Green) and *Grp*$^+$ (White) interneurons, yellow and white arrows indicate mWGA-mCherry double-labeled with *Npy* and *Grp*, respectively. **I** mWGA-mCherry signals were detected in *Npy*$^+$ (White), but only a few in *Grpr*$^+$ (Green) interneurons, yellow arrows indicate mWGA-mCherry double-labeled with *Npy*. **J** Quantification of mWGA-mCherry double-labeled *Grp* and *Grpr*. 9 and 6 spinal cord sections from 3 mice were analyzed, respectively, student's unpaired two-tailed *t* test. **K** Quantification of *Grp*$^+$ labeled HSV-mCherry in the SDH. 10 spinal cord sections from five mice were analyzed. **L** HSV-mCherry signals were detected in *Grp*$^+$ (White) interneurons, yellow and gray arrows indicate HSV-mCherry double-labeled with *Grp* and AAV helper, respectively. **M** Quantification of *Npy*$^+$ labeled RV-CVS-EnvA-ΔG-tdTomato in the SDH. 12 spinal cord sections from five mice were analyzed. **N** RV-CVS-EnvA-ΔG-tdTomato signals were detected in *Npy*$^+$ (White) interneurons, yellow and purple arrows indicate RV-CVS-EnvA-ΔG-tdTomato double-labeled with *Npy* and AAV helper, respectively. Cells containing ≥ 5 RNAscope puncta were considered positive expressions. Data are shown as means ± SEM. Scale bars and *P* values are indicated in the figures. Source data are provided as a Source Data file. Created in BioRender. Wang, Z. (2025) https://BioRender.com/8lt9u0c.

injected RV-CVS-EnvA-ΔG-tdTomato virus into the SDH in *Grp*^{Cre} mice (Fig. S5C). The double labeling of helper virus and *Grp*$^+$ neurons in *Grp*^{Cre} mice was used to confirm the specific virus infection (Fig. S5E). The results, by observing fluorescently labeled neurons and combining them with *Npy* RNAscope, confirmed the anatomical connection between the NPY$^+$ and GRP$^+$ interneurons (Figs. 4M, N and S5D). These data suggest that GRP$^+$ interneurons are the direct downstream interneurons of NPY$^+$ interneurons with monosynaptic connections.

Next, we examined whether *Npy1r* and *Grp* are expressed in the same population of interneurons in the SDH by RNAscope assay. The results showed that *Npy1r and Grp* mRNA expressions have remarkably high co-localization in the lamina II of SDH, with 66.93% of *Npy1r*$^+$ interneurons expressing *Grp* and 66.44% of *Grp*$^+$ interneurons expressing *Npy1r* (Fig. 5A, B). To determine the role of GRP$^+$ interneurons in morphine-induced itch, we used *Grp*^{Cre}*;iDTR* mice to ablate GRP$^+$ interneurons via intraperitoneal (i.p.) injections of diphtheria toxin (DTX). RNAscope results revealed that the number of *Grp*$^+$ neurons was dramatically decreased in the spinal cord of *Grp*^{Cre}*;iDTR* mice after DTX treatments (Fig. S6A, B, $t = 14.89$, $P < 0.0001$). Behavioral assay showed that morphine-induced itch was significantly attenuated in *Grp*^{Cre}*;iDTR* mice (Fig. 5C, $t = 3.155$, $P = 0.0058$; Fig. S6C, $t = 2.559$, $P = 0.0203$). Similarly, chemogenetic inhibition of GRP$^+$ interneurons by using *Grp*^{Cre}*;hM4Di* mice was also significantly suppressed in morphine-induced itch (Fig. 5D, $t = 2.552$, $P = 0.0190$) and biting and licking (Fig. S6D, $t = 2.791$, $P = 0.0113$) after CNO treatment. These data suggested that GRP$^+$ interneurons are required for morphine-induced itch. To examine whether GRP itself also participates in the morphine-induced itch, we generated GRP conditional knockout mice (*Vglut2*^{Cre}*;Grp*$^{fl/fl}$) by cross-breeding *Vglut2*^{Cre} mice with *Grp*$^{fl/fl}$ mice. Strikingly, conditional deletion of *Grp* in excitatory interneurons significantly decreased morphine-induced itch (Fig. 5E, $t = 3.283$, $P = 0.0033$). GRP$^+$ interneuron activation will release GRP, which acts on the GRPR to induce itch[12]. We found that intrathecal injected GRPR antagonist PD176252 (10 μg) significantly inhibits morphine-induced itch, indicating that GRPR is the downstream signaling of GRP$^+$ interneurons in this behavior (Fig. 5F, $t = 3.972$, $P = 0.0010$; Fig. S7A, $t = 2.617$, $P = 0.0180$). Given that GRPR$^+$ neurons were reported to be regulated by KOR in the spinal cord[38], we also tested the effects of KOR agonist nalfurafine (40 ng) on morphine-induced itch. Consistent with a previous study[32], we found that nalfurafine significantly blocked morphine-induced itch (Fig. S7B, $t = 6.901$, $P < 0.0001$, Fig. S7C, $t = 3.722$, $P = 0.0017$). Together, these results suggest that morphine-induced itch requires both GRP$^+$ interneurons and GRP.

MOR activation on NPY$^+$ interneurons disinhibits GRP$^+$ interneurons

To examine whether the GRP$^+$ interneurons receive inhibitory inputs from the MOR-expressing NPY$^+$ interneurons, we carried out an electrophysiological analysis of the effect of morphine on the spontaneous inhibitory postsynaptic currents (sIPSCs) in the lamina I-II GRP$^+$ interneurons by using *Grp*^{Cre};Ai9 mice, in which *Grp*$^+$ interneurons are genetically labeled by td-Tomato (Fig. S8A–C). Our recording data showed that perfusion of morphine (10 μM) notably decreased the frequency and amplitude of sIPSCs (Fig. 6A–D, $t = 6.457$, $P < 0.0001$, $t = 2.420$, $P = 0.0340$, respectively), which would be expected if morphine interacts with presynaptic MOR at NPY$^+$ neuron inputs. Morphine's inhibition of sIPSCs was not altered by BIBO3304 (Fig. S9A–C, $t = 8.759$, $P < 0.0001$; $t = 3.189$, $P = 0.0153$ for frequency and amplitude, respectively). Furthermore, morphine (10 μM) also significantly decreased the frequency and amplitude of miniature IPSCs in the presence of 0.5 μM TTX (Fig. 6G–I, $t = 4.111$, $P = 0.0012$; $t = 4.320$, $P = 0.0008$, respectively). Morphine did not show significant changes in sEPSC recorded from GRP$^+$ neurons (Fig. S9D–F, $t = 0.07768$, $P = 0.9389$; $t = 1.872$, $P = 0.0776$ for frequency and amplitude, respectively). But morphine evoked outward currents in 26% of GRP$^+$ neurons (Fig. S9G, H). These results show that morphine specifically inhibited the sIPSCs recorded from GRP$^+$ neurons, which suggests that GABA/Glycine participates in this inhibitory circuit. Moreover, the activity of GRP$^+$ interneurons in morphine-induced itch was examined by in vivo fiber photometry recording in *Grp*^{Cre}*;GCamp6f* mice (Fig. 6J, K). We found that GRP$^+$ interneurons are significantly activated after morphine injection, which is correlated with the scratching responses (Figs. 6K and S10A). In addition, co-injection of MOR antagonist naloxone (10 nmol) or NPY (10 μg) blocked the activation of GRP$^+$ interneurons by morphine (0.3 nmol) (Figs. 6K and S10B, C).

Furthermore, we examined whether NPY can directly impact the excitability of GRP$^+$ interneurons. NPY (10 μM) significantly increased rheobase and decreased the numbers of current injection-evoked action potentials in SDH lamina II GRP$^+$ interneurons (Fig. 7A–C, $t = 3.789$, $P = 0.0068$; $F(1, 7) = 15.13$, $P = 0.0060$). In contrast, vehicle perfusion did not change rheobase or action potentials (Fig. 7D–F, $t = 0.8018$, $P = 0.4433$, $F(1, 234) = 2.233$, $P = 0.1364$). Additionally, NPY (10 μM) perfusion evoked outward currents, which were blocked by BIBO3304 (2 μM), in the SDH lamina II GRP$^+$ interneurons with an average amplitude of 18.785 pA (Fig. 7G, $t = 6.803$, $P < 0.0001$). We then tested the effect of NPY on GRP$^+$ interneurons activation induced scratching behaviors. Chemogenetic activation of GRP$^+$ interneurons in *Grp*^{Cre}*;hM4Dq* mice with the CNO (10 nmol) elicited robust itch, which was entirely abolished by intrathecal injection of NPY (10 μg) (Fig. 7H, $t = 3.479$, $P = 0.0083$). These results suggest that NPY can directly inhibit the excitability of GRP$^+$ interneurons and suppress itch mediated by these neurons.

Discussion

Itch is a common side effect of opioid analgesics. In this study, we demonstrated that intrathecal μ-opioids, such as morphine and EM-1,

https://doi.org/10.1038/s41467-025-62382-w

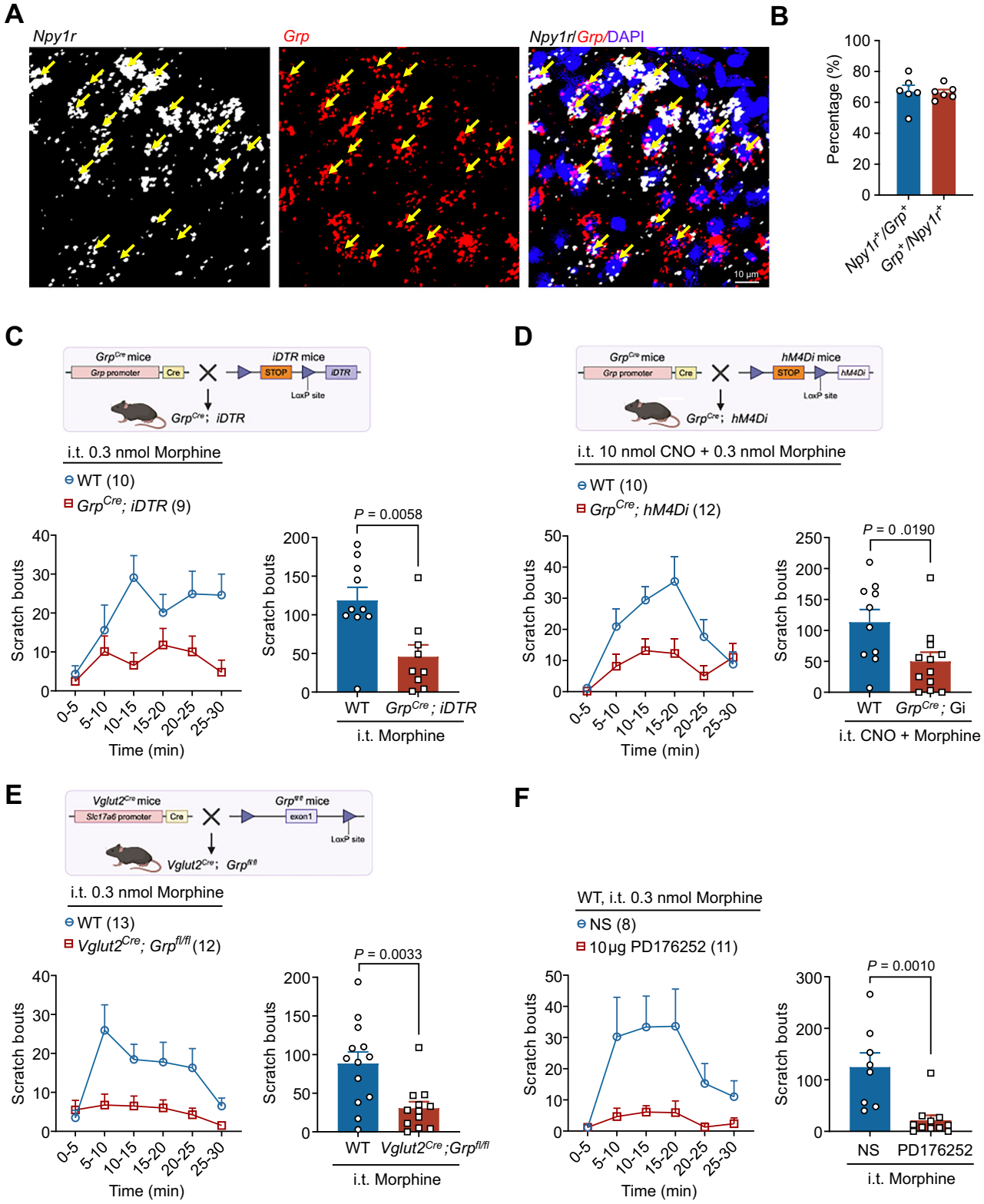

Fig. 5 | GRP⁺ interneurons and GRP are required for morphine-induced itch. A In situ hybridization RNAscope images of *Npy1r* (White) and *Grp* (red) mRNA in mouse SDH of WT mice, yellow arrows indicate *Npy1r* double labeled with *Grp*, Scale bar = 10 μm. **B** The percentage of co-expression between *Npy1r*⁺ and *Grp*⁺ neurons in SDH, 14 spinal cord sections from 6 mice were analyzed. **C** Morphine-induced itch was significantly inhibited in *Grp*^{Cre};*iDTR* mice, Diphtheria toxin (50 μg/kg, 5 μg/mL in sterile PBS) was intraperitoneal injected every other day, one week before intrathecal injected morphine (0.3 nmol), student's unpaired two-tailed *t*-test. **D** Morphine (0.3 nmol)-induced itch was significantly inhibited by chemogenetic inhibition *Grp*⁺ neurons in *Grp*^{Cre};*hM4Di* mice following CNO injection (10 nmol), student's unpaired two-tailed *t*-test. **E** Morphine (0.3 nmol)-induced itch was significantly inhibited in *Vglut2*^{Cre};*Grp*$^{fl/fl}$ mice. Student's unpaired two-tailed *t*-test. **F** Intrathecal morphine (0.3 nmol)-induced itch was inhibited by co-injection of GRPR antagonist PD176252 (10 μg) in WT mice, student's unpaired two-tailed *t*-test. Data are shown as means ± SEM. *P* values are indicated in the figures. Sample sizes are presented in parentheses. Source data are provided as a Source Data file. *Created in BioRender. Wang, Z. (2025)* https://BioRender.com/oklxfey.

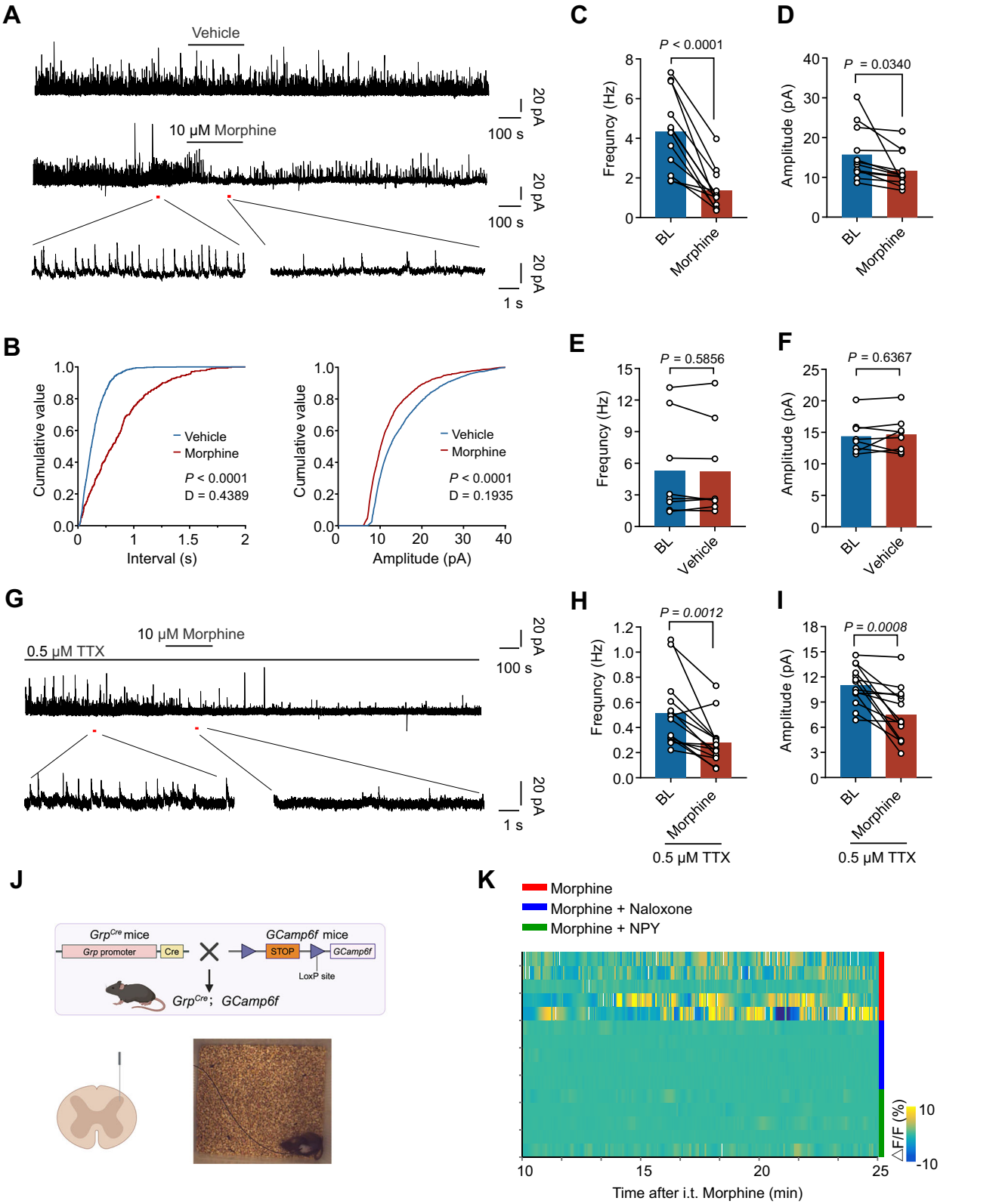

elicit itch responses mediated by MOR on spinal NPY$^+$ inhibitory interneurons. MOR activation inhibited the excitability of NPY$^+$ inhibitory interneurons in the spinal cord. Additionally, NPY$^+$ inhibitory interneurons provided direct monosynaptic inputs to GRP$^+$ interneurons and regulated the activities of GRP$^+$ interneurons via the NPY-NPY1R system. Finally, GRP$^+$ interneurons and GRP were required for morphine-induced itch. Together, our findings suggest that the activation of MOR on spinal NPY$^+$ inhibitory interneurons mediates opioid-induced itch by directly disinhibiting GRP$^+$ interneurons, as depicted in Fig. 8.

Recent progress has revealed new mechanisms and advanced our understanding of morphine-induced itch, suggesting that MOR on inhibitory interneurons mediated opioid-induced itch via disinhibition[4,32]. However, the subtype of inhibitory interneurons in

Fig. 6 | Morphine impairs inhibitory synaptic transmission in GRP$^+$ interneurons in the SDH. A Recording traces of spontaneous inhibitory postsynaptic currents (sIPSCs) after vehicle and morphine (10 μM) treatments in GRP$^+$ interneurons of the spinal slices from *Grp^{Cre};Ai9* mice. **B** Cumulative histograms of the inter-event interval and amplitude of sIPSCs after the vehicle and morphine treatments, $P < 0.0001$, respectively. two-tailed Kolmogorov-Smirnov test. **C** The sIPSC frequency before and after morphine treatment, 12 neurons from 5 mice were analyzed, paired two-tailed *t*-test. **D** The sIPSC amplitude before and after morphine treatment, 12 neurons from 5 mice were analyzed, $P = 0.0340$, paired two-tailed *t*-test. **E** The sIPSC frequency before and after vehicle treatment, 8 neurons from 4 mice were analyzed, paired two-tailed *t*-test. **F** The sIPSC amplitude before and after vehicle treatment, 12 neurons from 5 mice were analyzed, paired two-tailed *t*-test. Data are shown as means with dots. *P* values are indicated in the figures. **G** Recording traces of miniature IPSCs after morphine (10 μM) treatments in GRP$^+$ interneurons of the spinal slices from *Grp^{Cre};Ai9* mice in the presence of 0.5 μM TTX. **H** The miniature IPSC frequency before and after morphine treatment, 14 neurons from 4 mice were analyzed, paired two-tailed *t*-test. **I** The miniature IPSC amplitude before and after morphine treatment, 14 neurons from 4 mice were analyzed, paired two-tailed *t*-test. **J** Schematic representation of the *Grp^{Cre};GCamp6f* mice and spinal dorsal horn fiber photometry recording in vivo. **K** Heatmaps shows the calcium signals within the 10-25 min after drugs injection (i.t., 0.3 nmol morphine, 10 nmol naloxone + 0.3 nmol morphine, and 10 μg NPY + 0.3 nmol morphine), n = 5 mice per group. Source data are provided as a Source Data file. Created in BioRender. Wang, Z. (2025) https://BioRender.com/waectjd.

opioid-induced itch signaling and related neuronal circuits remains unclear. Here, we found that NPY$^+$ interneurons participate in the opioid-induced itch. Strikingly, MOR agonists-induced itch was completely lost in *Npy^{Cre};Oprm1$^{fl/fl}$*, as confirmed by three doses of morphine and MOR endogenous ligand EM-1. Our electrophysiology results demonstrated that morphine inhibits neuronal excitability of NPY$^+$ interneurons. Moreover, we found that chemogenetic activation of NPY$^+$ neurons abolished intrathecal morphine-induced itch. These results support and confirm that MOR activation on NPY$^+$ interneurons inhibits their excitability and mediates opioid-induced itch.

Notably, this study demonstrated that NPY and LP-NPY significantly inhibited opioid-induced itch, and this inhibitory effect was blocked by the pretreatment with an NPY1R antagonist or in *Npy1r$^{-/-}$* mice. These findings suggest that the NPY-NPY1R system and NPY1R$^+$ interneurons are essential in regulating opioid-induced itch. While involvement of NPY$^+$ and NPY1R$^+$ interneurons in itch regulation is well-documented, their specific roles in mediating chemical versus mechanical itch transmission remain debated[22,23,29]. Goulding et al. reported that NPY$^+$ interneurons ablation or chemogenetic inhibition elicited spontaneous itch and mechanical itch[24], and further revealed that NPY$^+$ interneurons gate NPY1R$^+$ interneurons to regulate mechanical itch transmission[23]. Additionally, several studies demonstrated that NPY-NPY1R system regulates not only mechanical itch but also chemical itch[21,29,30]. For instance, Gao et al. reported that the NPY1R selective agonist LP-NPY regulates both mechanical and histaminergic itch[29]. Boyle et al. reported that chemogenetic activation of NPY$^+$ interneurons reduces chloroquine-evoked non-histaminergic chemical itch[21]. Notably, our results demonstrate a remarkable co-localization (66%) of NPY1R and GRP in the SDH. This finding is further supported by Nelson et al., who reported that about 60% of NPY1R is colocalized with GRP in the SDH[39]. The GRP$^+$ interneurons and GRP-GRPR system have been demonstrated to mediate chemical itch at the spinal level[40–42]. Therefore, co-expression of NPY1R and GRP in the spinal interneurons suggests that chemical and mechanical itch may not be strictly separated by NPY1R or GRP neurons and may have some overlap via NPY1R and GRP co-expressed neurons. The GRP$^+$/NPY1R$^+$ neurons may participate in both chemical and mechanical itch, as well as in opioid induced itch. However, this study did not validate whether NPY1R and GRP co-expressed neurons regulate both chemical itch and mechanical itch. Future dedicated studies are needed to elucidate the detailed components of chemical or mechanical itch signaling pathways in GRP$^+$/NPY1R$^+$ neurons and opioid-induced itch.

NPY1R$^+$ interneurons have been demonstrated to receive synaptic contacts from NPY$^+$ interneurons[23]. Given that NPY1R is highly colocalized with GRP, we speculate that GRP$^+$ interneurons also receive synaptic inputs from NPY$^+$ interneurons. Indeed, the anterograde WGA tracing and HSV tracing from *Npy^{Cre}* mice indicated GRP$^+$ neurons receive direct synapse input from NPY$^+$ neurons. This is further confirmed by the RV retrograde tracing from *Grp^{Cre}* mice. The WGA tracing captured a few GRPR$^+$ neurons. Thus, we cannot exclude the possibility that NPY$^+$ neurons also synapse on the GRPR$^+$ neurons. Furthermore, NPY directly inhibited GRP$^+$ interneurons' excitability by evoking outward currents, increasing rheobase, and decreasing the action potentials. Combined with the results from NPY and LP-NPY, which significantly inhibit opioid-induced itch, and this inhibitory effect was blocked by the pretreatment with NPY1R antagonist or in *Npy1r$^{-/-}$* mice, indicating that decreased NPY-NPY1R signaling may play a major role in opioid-induced itch. This study also found that IPSCs recorded from GRP$^+$ neurons were significantly inhibited by morphine perfusion, which suggests that GABA/Glycine may also participate in this inhibitory effect, and future studies should evaluate the difference between NPY-mediated inhibition of GRP$^+$ neurons and GABA/glycine-mediated inhibition of GRP$^+$ neurons in the itch regulation. Taken together, these results reveal a previously undescribed inhibitory microcircuit in the SDH, where NPY$^+$ interneurons have direct inhibitory synaptic inputs to GRP$^+$ interneurons, which play a major role in opioid-induced itch.

Furthermore, the present study uncovered the critical roles of the GRP-GRPR pathway in opioid-induced itch. First, this study indicated that GRP$^+$ interneurons are required for morphine-induced itch, which has not yet been reported. Morphine-induced itch was dramatically decreased in the GRP$^+$ neurons-ablated mice (*Grp^{Cre};iDTR*) or by chemogenetic inhibition of GRP$^+$ interneurons in *Grp^{Cre};hM4Di* mice. Second, morphine-induced itch was decreased in GRP conditional knockout mice (*Vglut2^{Cre};Grp$^{fl/fl}$*), directly showing that GRP itself is essential for morphine-induced itch. Last, GRPR antagonist PD176252 significantly inhibited morphine-induced itch, which is consistent with previous results from GRPR knockout mice[31]. These results suggest both GRP$^+$ interneurons and GRP are necessary for morphine-induced itch.

GRPR$^+$ interneurons in the SDH have been demonstrated to be involved in opioid-induced itch[4,31]. For example, we found that ablation of GRPR$^+$ interneurons abolishes morphine-induced itch[4]. Liu et al. reported that knockout or pharmacological blockade of GRPR prevents morphine-induced scratching behaviors[31]. These studies confirm that GRPR$^+$ interneurons and GRPR contribute to opioid-induced itch. However, studies using in situ RNAscope and single-cell analysis in SDH neurons showed limited co-localization of *Oprm1* and *Grpr*[4,43]. This study shows that GRP$^+$ neurons and GRP itself are essential for morphine-induced itch. Thus, GRPR$^+$ neurons might be downstream of the pathway for morphine-induced itch. Nguyen et al. revealed that MOR on dynorphin$^+$ interneurons mainly mediates opioid-induced itch by disinhibition of *Oprk1*$^+$ neurons, and KOR agonist inhibited morphine-induced itch[32]. The *Oprk1*$^+$ neurons were demonstrated to overlap with GRPR$^+$ neurons in the spinal cord[38]. While disinhibition of GRPR neurons can trigger itch responses. However, this mechanism alone cannot fully explain certain observations at the molecular level, such as the loss of morphine-induced itch in *Grpr* knockout or knockdown mice and the inhibitory effects of GRPR antagonists on morphine-induced itch[44]. In the present study, we demonstrated that NPY$^+$ inhibitory interneurons mediate GRP$^+$ interneurons disinhibition, which functions upstream of GRPR$^+$ neurons in opioid-induced itch. This mechanism provides a reasonable explanation for the decrease of

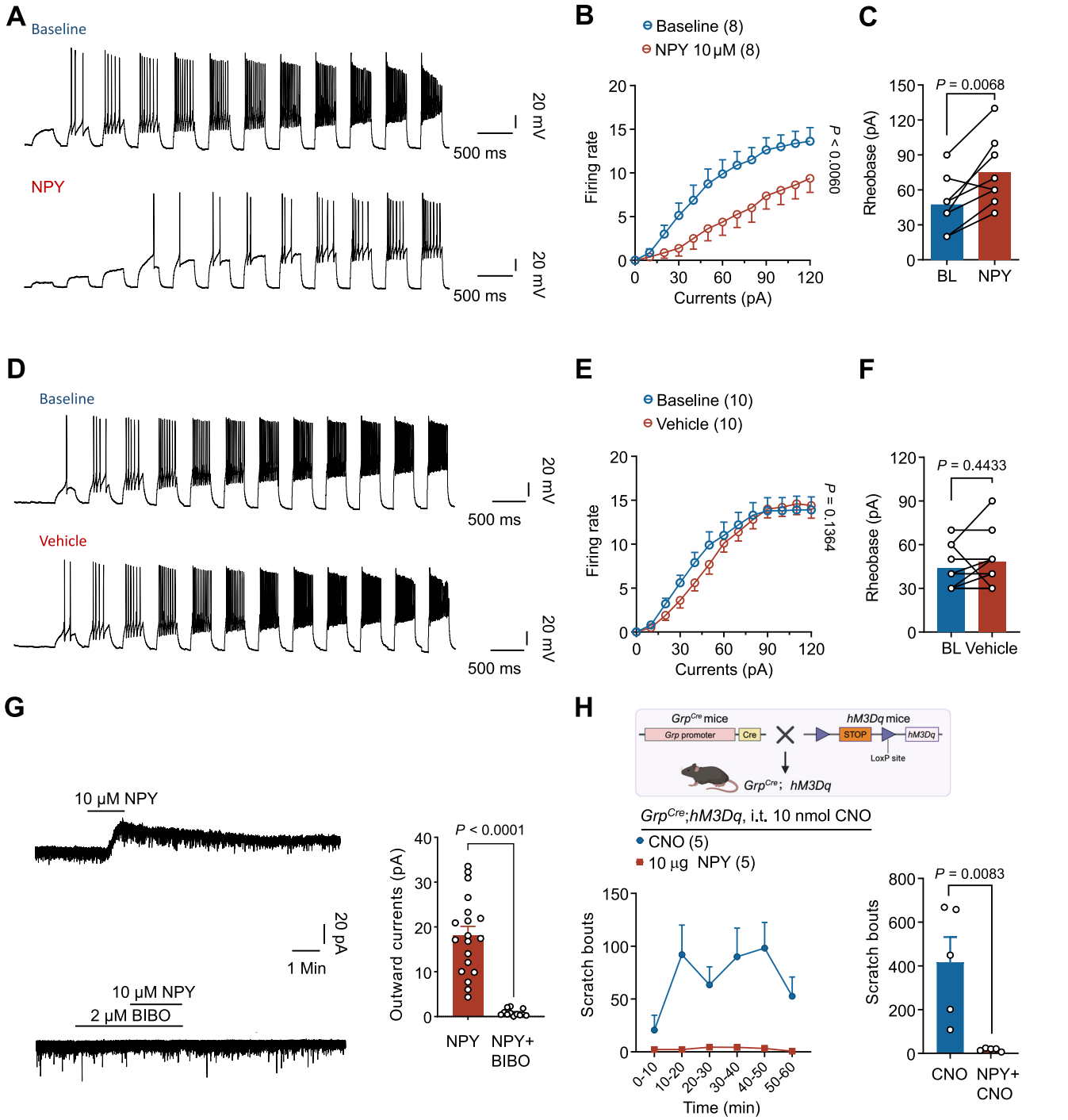

Fig. 7 | NPY regulates GRP$^+$ interneurons, and GRP$^+$ interneurons mediate itch responses. A Representative traces of action potentials before and after NPY (10 μM) treatment in GRP$^+$ interneurons in the spinal slices from *Grp^{Cre};Ai9* mice. **B** Quantifications of the effects of NPY on action potentials, two-way ANOVA, Bonferroni's multiple comparisons. 8 neurons from 3 mice were analyzed. **C** Quantifications of the rheobase, paired two-tailed *t*-test. 8 neurons from 3 mice were analyzed. **D** Representative traces of action potentials before and after vehicle treatment in *Grp*$^+$ interneurons in the spinal slices from *Grp^{Cre};Ai9* mice. **E** Quantifications of the effects of the vehicle on action potentials, two-way ANOVA, Bonferroni's multiple comparisons.10 neurons from 3 mice were analyzed. **F** Quantifications of the rheobase, paired two-tailed *t*-test. Data are shown as means with dots. 10 neurons from 3 mice were analyzed. **G** NPY (10 μM) induced outward currents were recorded and inhibited by BIBO3304(2 μM) from GRP$^+$ interneurons in the SDH from *Grp^{Cre};Ai9* mice. 19 neurons from 3 mice and 12 neurons from 3 mice were analyzed, respectively. Student's unpaired two-tailed *t*-test. **H** Time course (left) and total scratch bouts (right) following intrathecal CNO (10 nmol) and NPY (10 μg) injection in *Grp^{Cre};hM3Dq*, student's unpaired two-tailed *t*-test. Data are shown as means ± SEM. *P* values are indicated in the figures. Sample sizes are presented in parentheses. Source data are provided as a Source Data file. Created in BioRender. Wang, Z. (2025) https://BioRender.com/ox4ft8z.

morphine-induced itch through ablation of GRP neurons and knockout of GRP, as well as knockout, knockdown, or antagonism of GRPR.

There are limitations for this study by using *Npy^{Cre}*, *Grp^{Cre}*, *vGlut2^{Cre}* mice strains to permit manipulation of specific neuronal populations in the spinal cord. A drawback of this approach is that it can lead to lineages of neurons being manipulated because of developmental changes in gene expression compared to adult expression. Boyle et al. reported that neurons that transiently NPY-expressing cells during

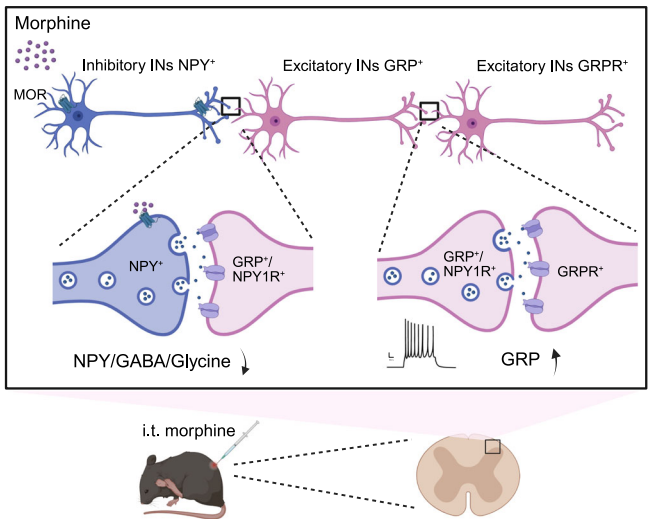

Fig. 8 | A schematic diagram illustrates the potential spinal neural circuits for morphine-induced itch. Morphine acts on MORs expressed on NPY$^+$ inhibitory interneurons and causes disinhibition of GRP$^+$/NPY1R$^+$ excitatory interneurons, then further activates GRPR$^+$ excitatory interneurons to elicit itch. Created in BioRender. Wang, Z. (2025) https://BioRender.com/os1fjsc.

development will also be manipulated by using *Npy*^{Cre} mouse line[21]. Secondly, besides the itch regulatory roles of NPY-NPY1R signaling, previous studies have also shown NPY-NPY1R signaling participates in pain transimition[21,39,45–47]. Nelson et al. reported that alleviation of neuropathic pain with NPY requires spinal GRP/NPY1R interneurons at the spinal level[39]. This is a similar pathway to that we reported in this study for opioid-induced itch. Future studies focusing on the similarities and differences of NPY-NPY1R signals in itch and pain regulation will be critical to elucidate their context-dependent mechanisms.

Methods

Animals

Oprm1$^{fl/fl}$ (stock No: 030074), *Npy*^{Cre} (stock No: 027851), *vGlut2*^{Cre} (stock No: 028863), *Grp* $^{fl/fl}$ (stock No: 033096), *Grp*^{Cre} (stock No:033174), Ai9-tdTomato (stock No: 007909), R26$^{iDTR/+}$ (stock No: 007900), R26$^{LSL\text{-}hM3Dq}$ (stock number: 026220), R26$^{LSL\text{-}hM4Di}$ (stock number: 026219), *GCamp6f* (stock number: 028865), and C57BL/6 J wild-type mice (stock No: 000664) were purchased from the Jackson Laboratory. *Npy1r*$^{-/-}$ mice (Strain NO. T006562) were purchased from GemPharmatech (Nanjing, China). All mice are maintained at the Southern University of Science and Technology Animal Facility. Mice at 1–2 months old, both sexes, were used for electrophysiological studies. Mice at 2–4 months, both sexes, were used for behavioral and pharmacological studies. Mice were group-housed on a 12-h light/12-h dark cycle at 22 ± 1 °C with free access to food and water. Sample sizes were estimated based on the previous studies for similar types of behavioral, biochemical, and electrophysiological assays and analyses[4]. Two to five mice were housed per cage. Animal studies were approved by the Institutional Animal Care and Use Committee of the Southern University of Science and Technology. Animal experiments were conducted in accordance with the National Institutes of Health Guide for the Care and Use of Laboratory Animals and ARRIVE guidelines. Experimenters were blind to drug treatments and subsequent experimentation and analyses.

Oprm1$^{fl/fl}$ mice were mated with *Npy*^{Cre} mice to obtain *Npy*^{Cre};*Oprm1*$^{fl/fl}$ mice with NPY positive neuron conditional knockout *Oprm1*. *Grp*$^{fl/fl}$ mice were mated with *vGlut2*^{Cre} mice to obtain *vGlut2*^{Cre};*Grp*$^{fl/fl}$ mice, which have the *Grp* conditionally knocked out in excitatory neurons. Condition knockout mice that are Cre-positive and flox homozygote F3 offspring. *Grp*^{Cre} mice were crossed with Ai9 mice, R26$^{LSL\text{-}hM4Di}$ mice, R26$^{LSL\text{-}hM3Dq}$ mice, R26$^{iDTR/+}$ mice, or *GCamp6f* mice to obtain *Grp*^{Cre};Ai9 mice, *Grp*^{Cre};*hM4Di* mice, *Grp*^{Cre};*hM3Dq* mice, *Grp*^{Cre};*iDTR* mice, or *Grp*^{Cre};*GCamp6f* mice respectively. *Npy*^{Cre} mice were crossed with Ai9 mice, R26$^{LSL\text{-}hM3Dq}$ mice, or R26$^{iDTR/+}$ mice to obtain *Npy*^{Cre};Ai9 mice, *Npy*^{Cre};*hM3Dq* mice, or *Npy*^{Cre};*iDTR* mice, respectively.

Drug injections

For intrathecal injections, lumbar puncture was made by a Hamilton microsyringe (Hamilton) fitted with a 30-G needle between the L5 and L6 spinal levels to deliver reagents (10 µl) into CSF in non-anesthetized mice. Puncture of the dura was indicated by a reflexive lateral flick of the tail or the formation of an 'S' shape by the tail[48]. The drugs included Morphine hydrochloride (China National Accord Medicines Corporation Ltd), Clozapine N-oxide (CNO; 16882, Cayman), NPY (MedChemExpress, HY-P0198A), BIBO3304 (MedChemExpress, HY-107725), Nalfurafine (MedChemExpress, HY-12745A), LP-NPY (MedChemExpress, HY-P1323A) EM-1 (MedChemExpress, HY-P0185), Naloxone (MedChemExpress, HY-17417), Diphtheria toxin (Sigma, D0564), PD176252 (MedChemExpress, HY-103286).

Behavioral assessment for itch response

Mice were individually habituated in small plastic chambers (14 × 18 × 12 cm) with metal meshed floors for one hour per day and habituated for injection advance 2 days. After injection, the behavior was video recorded for 30 or 60 min using a Sony camera. The video was subsequently played back and the bouts number of scratches for each mouse were quantified in a blinded manner. For the intrathecal injection experiments, all scratch bouts by hindpaws were counted. Most scratches toward the side of the back from the nape to the thoracic segments, as well as a few scratches to the facial area. Scratch bouts were counted when the mouse lifted its hind paw to scratch and then put its paw back to the floor or its mouth. For biting and licking behaviors, the duration of a mouse spent biting or licking the affected hind paw, or the tail was recorded[4].

RNAscope In situ hybridization

Animals were deeply anesthetized with avertin (120–150 µl/10 kg, intraperitoneally) and trans cardiac perfusion was performed with PBS, followed by 4% paraformaldehyde. After the perfusion, spinal cords were removed and post-fixed in 4% paraformaldehyde overnight at 4 °C. The tissues were then cryopreserved in 20% sucrose in PBS for 1 day followed by 30% sucrose in PBS for 1 day. Spinal cord sections (30 µm) were cut using a cryostat (Minux FS800, RWD). In situ hybridization was performed using an RNAscope® Multiplex Fluorescent Detection Reagents Kit v2 (Advanced Cell Diagnostics, 323110) following the manufacturer's protocol and our previous report[20,49]. Briefly, samples were incubated with hydrogen peroxide for 10 min at room temperature, then incubated with protease III at 40 °C for 30 min in the HybEZ Oven. Subsequently, hybridization of the RNA probes to the mRNA targets was performed by incubation for 2 h at 40 °C. The Multiplex Fluorescent Kit v2 protocol was followed using commercial probes for *Oprm1* (Mm-Oprm1-C3, Cat. 315841- C3), *Npy* (Mm-Npy, Cat.313321-C2), *Npy1r* (Mm-Npy1r, Cat.427021), *c-Fos* (Cat. 316921-C3), *Grp* (Mm-Grp, Cat. 317961-C2/317861-C3), and *Grpr* (Mm-Grpr, Cat. 317871). A fluorescence evaluation Kit from PerkinElmer (NEL741001KT, NEL744001KT, and NEL745001KT) was used for the fluorescence signals. After three rinses, all those sections were mounted using Fluoroshield™ containing DAPI (Sigma, F6057). Images were obtained using a multiphoton laser point scanning confocal microscopy system (Zeiss, LSM980, Carl Zeiss AG, Oberkochen, Germany) and analyzed with Zeiss ZEN 3.4 (blue edition) software. For quantification purposes, all images were acquired under the same settings. Two to three sections from each animal were selected, and more than three animals were included for each group in the data

analysis. Visualized cells with more than five puncta per cell were classified as positive neurons[4].

Real-time quantitative PCR (qPCR)

Total RNA was extracted from lumbar SDH tissue using an RNAsimple Total RNA Kit (TianGen, DP419) according to the manufacturer's instructions. cDNA was prepared from total RNA by reverse transcription reaction with PrimeScriptTM RT regent Kit with gDNA Eraser (Takara, RR047A). The q-PCR was performed with a qTOWER3 (Analytik Jena, Germany) using TB Green premix Ex Taq (Takara, RR820A). The conditions for fast qPCR were as follows: 1 cycle of 95 °C for 30 s, 40 cycles of 95 °C for 5 s, and 60 °C for 34 s. Primer sequences as shown in Table S2.

Spinal cord slice preparation and patch-clamp recordings

Spinal cord slice preparation and patch-clamp recordings were performed according to the previous study[50]. Mice were anesthetized with avertin (120–150 μl/10 kg, intraperitoneally), the lumbosacral spinal cord was quickly dissected, and the tissue was placed in ice-cold dissection solution (in mM: Sucrose 240, $NaHCO_3$ 25, KCl 2.5, $NaH_2PO_4{\cdot}2H_2O$ 1.25, $CaCl_2{\cdot}2H_2O$ 0.5, $MgCl_2{\cdot}6H_2O$ 3.5, Ascorbic acid 0.4, Sodium pyruvate 2), equilibrated with 95% O_2 and 5% CO_2. Mice were sacrificed by decapitation following spinal extraction under anesthesia. Transverse spinal slices (300-400 μm) were cut by using a vibrating microslicer (VT1200s Leica). The slices were incubated at 34 °C for 1 h in artificial CSF (in mM: NaCl 117, KCl 3.6, $NaH_2PO_4{\cdot}2H_2O$ 1.2, $CaCl_2{\cdot}2H_2O$ 2.5, $MgCl_2{\cdot}6H_2O$ 1.2, $NaHCO_3$ 25, Glucose 11, Ascorbic acid 0.4, Sodium pyruvate 2), equilibrated with 95% O_2 and 5% CO_2.

The slices were placed in a recording chamber and perfused at a flow rate of 2–4 ml/min with ACSF which was saturated with 95% O_2 and 5% CO_2 and maintained at room temperature[51]. Lamina II neurons in lumbar segments were identified as a translucent band under a microscope (Scientifica) with light transmitted from below. Npy^{Cre};Ai9 and Grp^{Cre};Ai9 mice were used for identified NPY^+ and GRP^+ interneurons. (1) Outward currents record: pipette solution contained (in mM): K-gluconate 135, KCl 5, $CaCl_2{\cdot}2H_2O$ 0.5, $MgCl_2{\cdot}6H_2O$ 2, HEPES 5, EGTA 5, Mg-ATP 5 (pH 7.4). Holding potential is −50 mV, gap free voltage-clamp were used recorded currents. (2) Action potential and rheobase recording: pipette solution is same as outward currents record. The current-clamp for action potential evoked by a set of gradually increasing currents (0–140 pA, 300 ms; in increments of 10 pA). Rheobase is evoked by a set of gradually increasing currents (0–140 pA, 30 ms; in increments of 10 pA), until product action potential. Holding potential is −70mV. (3) sEPSC recording: pipette solution is same as outward currents record. Holding potential is −70mV, gap free voltage-clamp were used recorded currents. (4) sIPSC record: The patch-pipette solution used to record sIPSCs contained (in mM): Cs_2SO_4 110, $CaCl_2{\cdot}2H_2O$ 0.5, TEA-Cl 5, $MgCl_2{\cdot}6H_2O$ 2, HEPES 5, EGTA 5, Mg-ATP 5 (pH 7.4). sIPSCs were recorded at a holding potential of 0 mV in voltage-clamp mode. The miniature IPSC was recorded in the presence of 0.5 μM Tetrodotoxin (TTX, Mreda, M046335). The patch-pipettes had a resistance of 6-8 MΩ. Signals were acquired using a HEKA amplifier. All drugs were bath applied by gravity perfusion via a three-way stopcock without any change to the perfusion rate.

sIPSC, mIPSC and sEPSC events were detected and analyzed using Mini Analysis Program version 6.0.7. Initially, the amplitude threshold was set at 6 and the area threshold at 15 for event detection. These thresholds were then adjusted to ensure that at least 90% of events were captured. Finally, manual verification was performed to confirm that all events were correctly identified.

Virus injection

Npy^{Cre} mice were anesthetized with isoflurane (3.5% for induction; 1.5–2% for surgery), and fixed to a stereoscope (RWD). To target neurons in the lumbar cord (L_4-L_6), we typically inject the spinal segments between T_{13}-L_1 vertebrae. Open the mouse's back skin around the hump, and confirm T_{13}-L_1 levels intervertebral space. Cut away the tissue that holds the vertebrae together to reveal the underlying spinal segments. Carefully puncture the meninges and peel them away, then the micropipette tip is positioned directly above the surface of the spinal segment to be injected. The micropipette should be 500 μm away from the midline, and gently lower the micropipette to a depth of 250 μm.

Wheat germ agglutinin (WGA) tracing

The Cre-dependent rAAV-CAG-DIO-mWGA-mCherry virus (BC-1227, BrainCase, 5.00×10^{12} vg/mL) was injected into the SDH (T_{13}-L_1 levels) of Npy^{Cre} mice to trace the post-synaptic neurons. Lumbar spinal cords were isolated for immunofluorescence 3–4 weeks after virus injection. We examined the co-localization of *Npy*, *Grp* and *Grpr* mRNA expressions by RNAscope assay and the WGA-mCherry signal in the SDH.

Herpes simplex virus (HSV) tracing

For anterogradely tracing the postsynaptic neurons of NPY^+ neurons, the spinal dorsal horn (T_{13}-L_1 levels) of Npy^{Cre} mice was injected by the helper viral mixture of rAAV-hSyn-DIO-EGFP-T2A-Her2CT9 (BC-1663, BrainCase, 2.00×10^{12} vg/mL) and rAAV-UL26.5-DIO-cmgD (BC-1356, BrainCase, 2.00×10^{12} vg/mL) in a volume ratio of 1:4. One month later, H129-dgD-hUbC-mCherry-P2A-scHer2::gD (BC-HSV-Hs06, BrainCase, 1.00×10^{8} vg/mL) was injected into the same injection site. The spinal cords were dissected 6 days later for RNAscope. We examined the co-localization of *Grp* mRNA expressions by RNAscope assay and the HSV-mCherry signal in the SDH.

Rabies virus (RV) tracing

For retrogradely tracing the presynaptic neurons of GRP^+ neurons, spinal dorsal horn injection (T_{13}-L_1 levels) of the helper mixture (the volume ratio is 1:2) of rAAV-EF1α-DIO-EGFP-T2A-TVA (BC-0041, BrainCase, 2.50×10^{12} vg/mL) and rAAV-EF1α-DIO-N2cG helper virus (BC-0442, BrainCase, 5.01×10^{12} vg/mL) was made 14 days ago, followed by RV-CVS-EnvA-ΔG-tdTomato virus (BC-RV-CVS, BrainCase, 5.00×10^{8} vg/mL) in Grp^{Cre} mice, the spinal cords were dissected 6 days later for RNAscope. We examined the co-localization of *Npy* mRNA expressions by RNAscope assay and the RV-tdTomato signal in the SDH.

In vivo fiber photometry recording

Grp^{Cre};*GCamp6f* mice were anesthetized with isoflurane (3.5% for induction; 1.5–2% for surgery) and the hair in the area around the hump at the back of the mice was shaved by using an electric shaver. An incision was made along the skin at the middle of the dorsal hump, and then connective tissue and muscles were gently removed, exposing the bones of the lumbar spinal segments. After the lumbar spinal columns were exposed, the mice were transferred to the stereotaxic apparatus. Adjust the mice and the arms of the stereotaxic manipulator such that the fiber optic cannulae (R-FOC-BL200C-39NA, ø1.25 mm, 200 μm Core, RWD) are positioned and touch the surface of the spinal cord and should 500 μm away from the midline. To record the neurons in the dorsal horn of the spinal cord, gently prick the mater attached to the spinal cord and lower the fiber optic cannulae to a depth of 250 μm. The ceramic ferrule securing a length of optic fiber was inserted into the hollow space of the ferrule. The ferrule was secured in place using denture base materials (430205, New Century Dental).

Mice were provided for 2 weeks to recover from the surgery. Mice were individually habituated in test cages for one hour per day and habituated for injection advance 2 days. At the beginning of the experiment, connect the patch cable with the fiber-optic implant by inserting both ceramic ferrules into the split sleeve until there is no gap between the surfaces of the ferrules. Then place the mice in the test cages for 30 min of habituation. Choose the 410 nm/470 nm excitation

light mode of the fiber photometry system (Tricolor Color Multichannel Fiber Photometry System—R821) and select 410 nm as the isosbestic control channel. Changes in fluorescence (△F/F) were calculated by smoothing signals from the isosbestic control channel to correct for movement artifacts and photo-bleaching. Before the formal experiment, preview the fluorescence data trace for 5–10 min to stabilize the fluorescence baseline. In the formal experiment, briefly anesthetize the mice with isoflurane, intrathecally inject morphine, and record for 30 min. During the recording process, manually mark the action as being triggered and identify the manual mark on the fluorescent signal when the mice were scratching[52].

Statistical analyses

All data were expressed as means ± SEM, and individual data points are shown for each graph. *N* values as indicated in the figure legends. Statistical analyses were completed with GraphPad Prism 9.0.0 (GraphPad Software, Inc., La Jolla, CA). Statistical data were analyzed using Student's *t* test (two groups), one- or two-way ANOVA (repeated measures over a time course), followed by Dunnett's multiple comparisons test or Bonferroni's multiple comparisons, respectively. The criterion for statistical significance was $P < 0.05$.

Reporting summary

Further information on research design is available in the Nature Portfolio Reporting Summary linked to this article.

Data availability

All data are available in the main text or the supplementary materials. Source data are provided with this paper.

References

1. Corder, G., Castro, D. C., Bruchas, M. R. & Scherrer, G. Endogenous and exogenous opioids in pain. *Annu. Rev. Neurosci.* **41**, 453–473 (2018).
2. Wang, Z. et al. Anti-PD-1 treatment impairs opioid antinociception in rodents and nonhuman primates. *Sci. Transl. Med.* **12**, eaaw6471 (2020).
3. Schmid, C. L. et al. Bias factor and therapeutic window correlate to predict safer opioid analgesics. *Cell* **171**, 1165–1175.e1113 (2017).
4. Wang, Z. et al. Central opioid receptors mediate morphine-induced itch and chronic itch via disinhibition. *Brain* **144**, 665–681 (2021).
5. Wang, Z. et al. Spinal DN-9, a peptidic multifunctional opioid/neuropeptide FF agonist produced potent nontolerance forming analgesia with limited side effects. *J. Pain.* **21**, 477–493 (2020).
6. Strang, J. et al. Opioid use disorder. *Nat. Rev. Dis. Prim.* **6**, 3 (2020).
7. Reich, A. & Szepietowski, J. C. Opioid-induced pruritus: an update. *Clin. Exp. Dermatol.* **35**, 2–6 (2010).
8. Kumar, K. & Singh, S. I. Neuraxial opioid-induced pruritus: an update. *J. Anaesthesiol. Clin. Pharm.* **29**, 303–307 (2013).
9. Brune, A., Metze, D., Luger, T. A. & Stander, S. Antipruritic therapy with the oral opioid receptor antagonist naltrexone. Open, non-placebo controlled administration in 133 patients. *Hautarzt* **55**, 1130–1136 (2004).
10. Kwatra, S. G., Stander, S. & Kang, H. PD-1 blockade-induced pruritus treated with a Mu-opioid receptor antagonist. *N. Engl. J. Med.* **379**, 1578–1579 (2018).
11. Murray-Brown, F. L. Naltrexone for cholestatic itch: a systematic review. *BMJ Support Palliat. Care* **11**, 217–225 (2021).
12. Chen, X. J. & Sun, Y. G. Central circuit mechanisms of itch. *Nat. Commun.* **11**, 3052 (2020).
13. Cevikbas, F. & Lerner, E. A. Physiology and pathophysiology of itch. *Physiol. Rev.* **100**, 945–982 (2020).
14. Sheahan, T., Warwick, C., Fanien, L. & Ross, S. The neurokinin-1 receptor is expressed with gastrin-releasing peptide receptor in spinal interneurons and modulates itch. *J. Pain.* **22**, 578–578 (2021).
15. Polgár, E. et al. expression defines a population of superficial dorsal horn vertical cells that have a role in both itch and pain. *Pain* **164**, 149–170 (2023).
16. Mishra, S. K. & Hoon, M. A. The cells and circuitry for itch responses in mice. *Science* **340**, 968–971 (2013).
17. Huang, J. et al. Circuit dissection of the role of somatostatin in itch and pain. *Nat. Neurosci.* **21**, 707 (2018).
18. Sun, Y. G. & Chen, Z. F. A gastrin-releasing peptide receptor mediates the itch sensation in the spinal cord. *Nature* **448**, 700–U710 (2007).
19. Sun, Y. G. et al. Cellular basis of itch sensation. *Science* **325**, 1531–1534 (2009).
20. Xu, K. et al. Cannabinoid CB2 receptor controls chronic itch by regulating spinal microglial activation and synaptic transmission. *Cell Rep.* **44**, 115559 (2025).
21. Boyle, K. A. et al. Neuropeptide Y-expressing dorsal horn inhibitory interneurons gate spinal pain and itch signalling. *Elife* **12**, RP86633 (2023).
22. Pan, H. et al. Identification of a spinal circuit for mechanical and persistent spontaneous itch. *Neuron* **103**, 1135–1149.e1136 (2019).
23. Acton, D. et al. Spinal neuropeptide y1 receptor-expressing neurons form an essential excitatory pathway for mechanical itch. *Cell Rep.* **28**, 625–639 e626 (2019).
24. Bourane, S. et al. Gate control of mechanical itch by a subpopulation of spinal cord interneurons. *Science* **350**, 550–554 (2015).
25. Kardon, A. P. et al. Dynorphin acts as a neuromodulator to inhibit itch in the dorsal horn of the spinal cord. *Neuron* **82**, 573–586 (2014).
26. Cui, H. A. et al. Lack of spinal neuropeptide Y is involved in mechanical itch in aged mice. *Front. Aging Neurosci.* **13**, 654761 (2021).
27. Smith, K. M., Nguyen, E. & Ross, S. E. The delta-opioid receptor bidirectionally modulates itch. *J. Pain.* **24**, 264–272 (2023).
28. Wang, Z. L., Donnelly, C. R. & Ji, R. R. Scratching after stroking and poking: a spinal circuit underlying mechanical itch. *Neuron* **103**, 952–954 (2019).
29. Gao, T. et al. The neuropeptide Y system regulates both mechanical and histaminergic itch. *J. Invest. Dermatol.* **138**, 2405–2411 (2018).
30. Chen, S. H. et al. Mechanical and chemical itch regulated by neuropeptide Y-Y signaling. *Mol. Pain.* **20**, 17448069241242982 (2024).
31. Liu, X. Y. et al. Unidirectional cross-activation of GRPR by MOR1D uncouples itch and analgesia induced by opioids. *Cell* **147**, 447–458 (2011).
32. Nguyen, E. et al. Morphine acts on spinal dynorphin neurons to cause itch through disinhibition. *Sci. Transl. Med.* **13**, eabc3774 (2021).
33. LaMotte, R. H., Dong, X. & Ringkamp, M. Sensory neurons and circuits mediating itch. *Nat. Rev. Neurosci.* **15**, 19–31 (2014).
34. North, R. A. & Williams, J. T. On the potassium conductance increased by opioids in rat locus coeruleus neurones. *J. Physiol.* **364**, 265–280 (1985).
35. Tsai, N. Y. et al. Trans-Seq maps a selective mammalian retinotectal synapse instructed by Nephronectin. *Nat. Neurosci.* **25**, 659 (2022).
36. Braz, J. M., Rico, B. & Basbaum, A. I. Transneuronal tracing of diverse CNS circuits by Cre-mediated induction of wheat germ agglutinin in transgenic mice. *Proc. Natl. Acad. Sci. USA* **99**, 15148–15153 (2002).
37. Cai, B. et al. A direct spino-cortical circuit bypassing the thalamus modulates nociception. *Cell Res.* **33**, 775–789 (2023).
38. Munanairi, A. et al. Non-canonical opioid signaling inhibits itch transmission in the spinal cord of mice. *Cell Rep.* **23**, 866–877 (2018).
39. Nelson, T. S. et al. Alleviation of neuropathic pain with neuropeptide Y requires spinal interneurons that coexpress. *JCI Insight* **8**, e169554 (2023).

40. Pagani, M. et al. How gastrin-releasing peptide opens the spinal gate for itch. *Neuron* **103**, 102 (2019).
41. Albisetti, G. W. et al. Dorsal Horn gastrin-releasing peptide expressing neurons transmit spinal itch but not pain signals. *J. Neurosci.* **39**, 2238–2250 (2019).
42. Sun, S. H. et al. Leaky gate model: intensity-dependent coding of pain and itch in the spinal cord. *Neuron* **93**, 840 (2017).
43. Haring, M. et al. Neuronal atlas of the dorsal horn defines its architecture and links sensory input to transcriptional cell types. *Nat. Neurosci.* **21**, 869–880 (2018).
44. Chen, Z. F. A neuropeptide code for itch. *Nat. Rev. Neurosci.* **22**, 758–776 (2021).
45. Tashima, R. et al. A subset of spinal dorsal horn interneurons crucial for gating touch-evoked pain-like behavior. *Proc. Natl. Acad. Sci. USA* **118**, e2021220118 (2021).
46. Nelson, T. S. et al. Spinal neuropeptide Y Y1 receptor-expressing neurons are a pharmacotherapeutic target for the alleviation of neuropathic pain. *Proc. Natl. Acad. Sci. USA* **119**, e2204515119 (2022).
47. Solway, B., Bose, S. C., Corder, G., Donahue, R. R. & Taylor, B. K. Tonic inhibition of chronic pain by neuropeptide Y. *Proc. Natl. Acad. Sci. USA* **108**, 7224–7229 (2011).
48. Hylden, J. L. K. & Wilcox, G. L. Intrathecal morphine in mice - a new technique. *Eur. J. Pharm.* **67**, 313–316 (1980).
49. Chen, G. et al. PD-L1 inhibits acute and chronic pain by suppressing nociceptive neuron activity via PD-1. *Nat. Neurosci.* **20**, 917–926 (2017).
50. Shan, L. et al. Injured sensory neurons-derived galectin-3 contributes to neuropathic pain via programming microglia in the spinal dorsal horn. *Brain Behav. Immun.* **117**, 80–99 (2024).
51. Jiang, C. Y., Fujita, T. & Kumamoto, E. Synaptic modulation and inward current produced by oxytocin in substantia gelatinosa neurons of adult rat spinal cord slices. *J. Neurophysiol.* **111**, 991–1007 (2014).
52. Schlegel, F. et al. Fiber-optic implant for simultaneous fluorescence-based calcium recordings and BOLD fMRI in mice. *Nat. Protoc.* **13**, 840–855 (2018).

Acknowledgements

This work was supported by the Department of Science and Technology of Guangdong Province (Key Area Research and Development Program of Guangdong Province: 2023B0303010002 to Z.W., 2023A1515011636 to Z.W. and 2021QN020751 to Z.W.), Shenzhen Medical Research Funding (C2301006 to Z.W. and C.W. and B2402043 to Z.W.), Shenzhen Science and Technology Program (20231120133942002 to Z.W. and JCYJ20220818103206013 to Z.W. and C.J.), and the National Natural Science Foundation of China (82101297 to Z.W.). We thank Dr. Yong Chen for advising and editing the manuscript. We thank the Southern University of Science and Technology Animal Facility for supporting animal experiments. We thank the Southern University of Science and Technology Core Research Facilities.

Author contributions

Conceptualization: Z.W., C.J. Methodology: Q.Z., Y. LI, Y.W., J.W., K.X., Y.C., Y.R., Y. Luo, and N.L. Investigation: Q.Z., Y. LI, Y.W., J.W., K.X., Y.C., Y.R., Y. Luo, and N.L. Visualization: Q.Z., Y. LI, Y.W., J.W., K.X., Y.C., Y.R., Y. Luo, and N.L. Supervision: Z.W., C.J., and C.W. Writing—original draft: Q.Z., and Z.W. Writing—review & editing: Q.Z., Z.W., C.J., and C.W.

Competing interests

The authors declare no competing interests.

Additional information

Supplementary information The online version contains supplementary material available at https://doi.org/10.1038/s41467-025-62382-w.

Correspondence and requests for materials should be addressed to Changyu Jiang, Chaoran Wu or Zilong Wang.

Peer review information *Nature Communications* thanks the anonymous reviewer(s) for their contribution to the peer review of this work. A peer review file is available.